

## Reflection ( $e,2e$ ) spectroscopy on surfaces

S. Iacobucci

*Istituto Metodologie Avanzate Inorganiche, Consiglio Nazionale Ricerche, Cassella Postale 10, I-00016 Monterotondo, Italy*

L. Marassi

*Dipartimento di Fisica, Università di Modena, via Campi, 213/A, I-41100 Modena, Italy*

R. Camilloni

*Istituto Metodologie Avanzate Inorganiche, Consiglio Nazionale Ricerche, Cassella Postale 10, I-00016 Monterotondo, Italy*

S. Nannarone

*Dipartimento di Fisica, Università di Modena, via Campi, 213/A, I-41100 Modena, Italy*

G. Stefani\*

*Dipartimento di Fisica "E. Amaldi," Terza Università di Roma, via C. Segre 2, I-00146 Roma, Italy*

(Received 30 January 1995)

This work reports a successful electron-electron coincidence experiment performed in grazing-angle reflection geometry. ( $e,2e$ ) measurements with a 300-eV impact energy have been carried out on a clean highly oriented pyrolytic graphite surface and the feasibility of binding-energy spectroscopy with quasimomentum discrimination has been established. Evidence is given that direct impact ionization of the valence electrons is the dominant ionization mechanism in the highly asymmetric kinematics used here.

Over the past twenty years ( $e,2e$ ) spectroscopy has developed as a well-established technique to investigating binding energies and momentum densities in atoms and molecules.<sup>1</sup> The application of ( $e,2e$ ) to solid samples, although begun in the earliest stages of the development of such a spectroscopy,<sup>2,3</sup> has been extensively investigated only during the past few years.<sup>4</sup> The applicability to surfaces has just started to be pursued and is still considered an open question.<sup>5-7</sup> This work proves that, working in grazing angle reflection geometry, pairs of coincident electrons correlated in energy and originating from the first layers of a highly oriented pyrolytic graphite (HOPG) surface can be detected and interpreted as the products of direct electron impact ionization of valence electrons.

An ( $e,2e$ ) experiment amounts to ionizing a target with an electron of well-defined energy and momentum  $E_0$  and  $\mathbf{k}_0$  and to measuring correlated in time the probability distribution of pairs of electrons exiting with energy and momentum  $E_s$  and  $\mathbf{k}_s$ ,  $E_e$  and  $\mathbf{k}_e$  within the solid angles  $d\Omega_s$  and  $d\Omega_e$ . Depending on the amount of the momentum transfer  $\mathbf{k}=\mathbf{k}_0-\mathbf{k}_s$ , two approximations can be used to describe the ( $e,2e$ ) process. In the dipolar limit,  $\mathbf{k}\sim\mathbf{0}$ , the ( $e,2e$ ) mechanism is equivalent to photoionization<sup>8</sup> and binding-energy spectroscopy is possible, while in the impulsive (binary) limit,  $\mathbf{k}\sim\mathbf{k}_e$ , the spectral momentum density of the electron bound in the target can also be measured.<sup>9</sup> Several experiments performed on gaseous targets have shown that the impulsive conditions can be satisfied both in symmetric ( $E_s=E_e$ ) and asymmetric ( $E_s>E_e$ ) kinematics; hence both kinematics permit measurement of momentum distributions.<sup>10</sup>

As far as application to solids is concerned, ( $e,2e$ ) experiments have been performed in transmission mode (which is

mainly bulk sensitive) using symmetric kinematics.<sup>2,11-15</sup> Recently, momentum spectroscopy in transmission geometry has been performed on amorphous C and HOPG upon asymmetric kinematics.<sup>6</sup> All of these experiments were aimed at measuring momentum densities. For the sake of completeness it is to be mentioned that experiments to investigate the dynamics of secondary electron emission have been performed on graphite and Si, measuring the low-energy secondary electrons ejected in backward direction (but unresolved in angle) in coincidence with the fast forward scattered electron.<sup>16,17</sup> To the best of our knowledge, the only successful attempt to observe electron-electron coincidence events from surfaces has been reported by Kirschner, Artamov, and Terekhov.<sup>5</sup> However, the feasibility of energy eigenvalues and momentum spectroscopy was not proven, due to the lack of information on the energies of the final electrons.

In this paper we present a successful attempt to perform an ( $e,2e$ ) experiment under reflection kinematics and at glancing incidence. The results are interpreted in terms of solid band structure,  $\epsilon(\mathbf{q})$ . The reflection geometry was originally studied by D'Andrea and Del Sole<sup>18</sup> in order to theoretically investigate the potentiality of the ( $e,2e$ ) spectroscopy on surfaces. The coincidence cross section in this arrangement is expected to depend strongly on the surface condition. Hence the measurement of momentum distribution of electronic states, which is peculiar to the impulsive ( $e,2e$ ) cross section, should give a relevant contribution to the understanding of surface properties.

To describe the ionization in the reflection kinematics, a further interaction besides the inelastic event must be considered in the collision, causing the incident electron with momentum  $\mathbf{k}_0$  to be elastically reflected along the specular

direction with momentum  $\mathbf{k}'_0$ .<sup>19</sup> An angle-resolved electron energy loss (AREEL) experiment<sup>20</sup> has shown that grazing angle electron scattering from HOPG is well described by this scattering model.

$$\frac{d^6\sigma}{d\Omega_s d\Omega_e dE_s dE_e} \propto \frac{k_s k_e}{k'_0} \left| \sum_t \int e^{-i\mathbf{k}_s \cdot \mathbf{r}_0} e^{-i\mathbf{k}_e \cdot \mathbf{r}_t} \prod_{j=1, j \neq t}^{N-1} \Psi_{\mathbf{q}}(\mathbf{r}_j) \frac{1}{|\mathbf{r}_0 - \mathbf{r}_t|} e^{i\mathbf{k}'_0 \cdot \mathbf{r}_0} \prod_{j=1}^N \Psi_{\mathbf{q}}(\mathbf{r}_j) d\mathbf{r}_0 d\mathbf{r}_1 \cdots d\mathbf{r}_N \right|^2 \times \delta(E_0 + \epsilon(\mathbf{q}) - E_s - E_e), \quad (1)$$

where  $t$  and  $j$  are valence electron indexes and  $\Psi_{\mathbf{q}}(\mathbf{r}_j)$  is a one-electron Bloch function with energy  $\epsilon(\mathbf{q})$  and crystal momentum  $\mathbf{q}$ . In the quasi-free-electron model, it can be written as a superposition of plane waves:

$$\Psi_{\mathbf{q}}(\mathbf{r}_j) = \sum_{\mathbf{G}} C_{\tilde{\mathbf{q}}-\mathbf{G}} e^{i(\tilde{\mathbf{q}}-\mathbf{G}) \cdot \mathbf{r}_j}, \quad (2)$$

where  $\mathbf{G}$  is a reciprocal lattice vector and  $\tilde{\mathbf{q}}$  is the momentum in the first Brillouin zone. Under the “frozen-core” assumption, the cross section becomes

$$\frac{d^6\sigma}{d\Omega_s d\Omega_e dE_s dE_e} \propto \frac{k_s k_e}{k'_0} \frac{1}{k'^4} \sum_{\mathbf{G}} |C_{\tilde{\mathbf{q}}-\mathbf{G}}|^2 \delta(E_0 + \epsilon(\mathbf{q}) - E_s - E_e), \quad (3)$$

where the momentum conservation

$$\mathbf{q} = \tilde{\mathbf{q}} - \mathbf{G} = \mathbf{k}' - \mathbf{k}_e \quad (4)$$

selects the coefficient  $C_{\tilde{\mathbf{q}}-\mathbf{G}}$  to be retained, being  $\mathbf{k}' = \mathbf{k}'_0 - \mathbf{k}_s$ .

It can be readily seen that for valence electrons, the ( $e,2e$ ) experiments can provide a momentum spectroscopy whenever the recoil momentum of the target is identifiable with the single-electron crystal momentum. Surface sensitivity, not intrinsically a property of the ( $e,2e$ ) cross section, is guaranteed by the reflection arrangement and enhanced by the glancing incidence kinematics.<sup>20</sup> Further surface sensitivity comes from the kinetic energy of the fast electrons ( $\sim 300$  eV) implying escape depths close to minimum.

The apparatus permits us to work at grazing incidence ( $\theta_0 = 0^\circ - 17^\circ$ ) (Fig. 1); details on the layout and on calibration measurements, both in the coincidence and noncoincidence counting mode, are reported elsewhere.<sup>22</sup> The equipment is based on an ultrahigh vacuum chamber containing an electron gun whose energy is automatically scanned during the experiment, a sample holder mounted on a temperature controlled manipulator with five degrees of freedom, and two electron analyzers. The emitted electrons were analyzed by a single-pass cylindrical mirror analyzer (CMA) (resolving power 50, angular acceptance  $\approx 0.23$  sr) with the axis coincident with the surface normal. The fast electrons were analyzed by a hemispherical deflector (HDA) equipped with a three element electrostatic lens, rotatable in the scattering

plane ( $\theta_s = 0^\circ - 12^\circ$ ) with an angular acceptance of  $\pm 0.5^\circ$ . It was operated at low-energy resolution (resolving power  $\sim 10^2$ ) in order to maximize the luminosity of the coincidence spectrometer. The overall energy resolution (3 eV) was mostly limited by this parameter.

The coincidence electronic chain is a conventional one.<sup>1</sup> The time resolution of the spectrometer is about 12 ns and is mostly determined by the time spread of the trajectories in the two analyzers. The “true” coincidence rate  $I_t$  must be distinguished from the nearly flat background of the uncorrelated events (“false” coincidences) which occurs at rate  $I_f$ . The optimal acquisition time is achieved when the ratio  $I_t/I_f$ , which depends on the incident current  $I_0$ , is about one.<sup>1</sup> In the best case we measured  $I_t \approx 0.05$  Hz with a ratio  $I_t/I_f \approx 0.5$  for  $I_0 \approx 1$  nA.

The HOPG sample was prepared according to UHV standard procedures<sup>23</sup> by peeling in air and annealing at about  $700^\circ\text{C}$  at a residual pressure of  $1 \times 10^{-10}$  mbar. Cleanliness and orientation of the surface were checked by Auger electron spectroscopy and AREEL measurements. The best monitor for surface cleanliness was the persistence of the sharp  $\pi \rightarrow \pi^*$  transition at 6.2 eV in the AREEL spectrum and the presence of a narrow angular distribution (FWHM =  $2.3^\circ$ ) of the elastic peak centered around the specular reflection direction ( $\theta_0 = \theta_s = 7^\circ$ ).<sup>20</sup> Reproducibility of these measurements over a period of six weeks has been assumed as a guarantee for the stability of the surface conditions and of the energy calibration during the long acquisition time necessary for coincidence measurements.

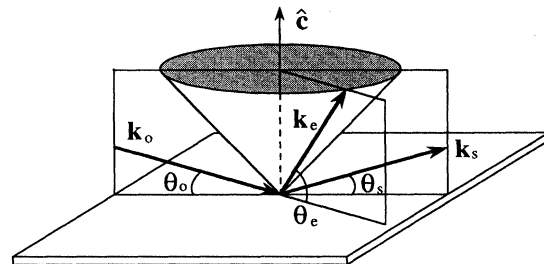


FIG. 1. Kinematics of the experiment.  $\mathbf{k}_0$  momentum of the incident electron,  $\mathbf{k}_s$  momentum of the scattered electron collected by the HDA in reflection geometry,  $\mathbf{k}_e$  momentum of the ejected electron lying on the cone surface collected by the CMA.

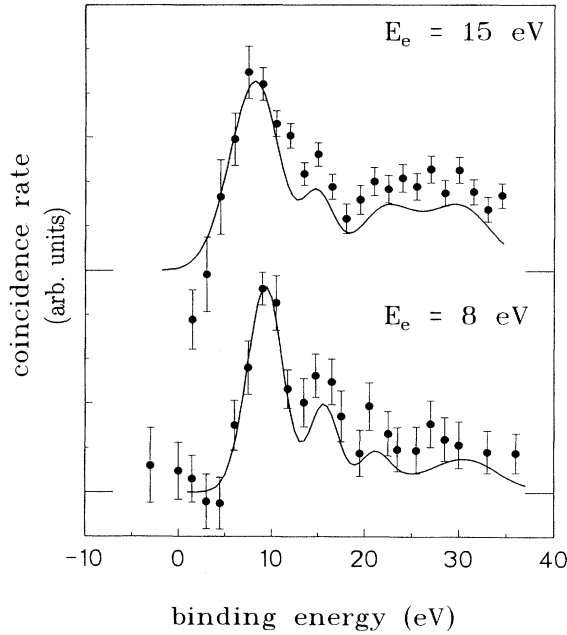


FIG. 2. Coincidence spectra from HOPG surface. Error bars represent one standard deviation for raw data. Fit of the spectra after multiple loss corrections are reported with continuous lines.

Coincidence spectra were measured by detecting the fast scattered electron around the specular direction at  $E_s = 300$  eV, correlated in time with the slow ejected electron of kinetic energies  $E_e = 8$  eV and  $E_e = 15$  eV while scanning  $E_0$ . The two sets of measurements have been reported on a common binding-energy (BE) scale by the energy balance  $\epsilon(\mathbf{q}) = E_0 - E_s - E_e$  established by Eq. (1). The coincidence spectra are reported in Fig. 2 together with the corresponding profiles as obtained after the multiple scattering correction described below.

Under the assumptions used to derive the cross section in Eq. (3), the features in the coincidence spectra have to be interpreted in terms of ionization events from valence bound states. The momentum  $\mathbf{q}$ , reconstructed according to Eq. (4), has nonvanishing components both in the parallel and perpendicular directions to the HOPG  $c$  axis ( $q_{\parallel}$  and  $q_{\perp}$ ); the computed values are reported in Table I. Assuming a three-

step model to describe the emission of the electron from the sample,<sup>24</sup> the presence of the surface potential will result in a change of the  $q_{\parallel}$  component. The voltage drop between target and spectrometer (estimated from the secondary binding electrons cutoff) was taken into account in calculating binding energies and effective  $q_{\parallel}$  values. Taking into account the finite analyzers' angular acceptances, the reconstructed component  $q_{\perp}$  ranges from nearly the middle to the boundaries of the first Brillouin zone in the  $\Gamma MK$  plane ( $\Gamma M$  and  $\Gamma K$  directions are averaged in HOPG).

Stemming from valence-band calculations<sup>25</sup> and on the basis of the values of momenta kinematically allowed, three individual contributions from valence states are to be expected in the measured spectra. In order to assign the binding energies the spectra were fitted by a least-squares method, simulating the three expected contributions by means of three Gaussian functions of variable height, width, and position. To achieve an acceptable fit, a fourth Gaussian, much broader than the others, had to be used to simulate the distribution at high binding energies.

Experimental data for  $(e,2e)$  on solid samples are affected by multiple losses that result in enhanced transition intensities at larger BE. In the present case the multiple losses probability for the fast electron,  $P(E_s)$ , is higher than for the slower one,  $P(E_e)$ . Their ratio can be written

$$P(E_e)/P(E_s) = \frac{l_e \lambda_s}{\lambda_e l_s} = \frac{1}{\lambda_e} \frac{d}{\sin \theta_e} \left( \frac{1}{\lambda_s} \frac{2d}{\sin \theta_s} \right)^{-1},$$

where  $l_e$  and  $l_s$  are the lengths traveled by the two electrons,  $\theta_e \approx 45^\circ$  and  $\theta_s = 7^\circ$  are the take-off angles, and  $d$  is the depth (the same for the two electrons) at which the coincidence event takes place. The mean free paths of the free electrons are estimated to be  $\lambda_e \sim 50$  Å and  $\lambda_s \sim 5$  Å.<sup>26</sup> Consequently  $P(E_e)/P(E_s) < 10^{-2}$  and the multiple scattering contribution in the ejected electron channel is negligible. In order to correct the coincidence spectrum for multiple losses, an AREEL spectrum was taken in the same conditions of the coincidence experiment and then subtracted from the raw data after normalizing the elastic peak to the intensity of the parent  $(e,2e)$  peak. The procedure was sequentially applied to all four of the contributions of the observed spectra. The correction results in a reduction of the coincidence rate for increasing BE, while the energy positions and the widths of

TABLE I. Momentum transfer  $K$ , momentum components with respect to the  $c$  axis of HOPG, and measured binding energies relative to the vacuum level (BE) and to the Fermi level (BE\*) for the four peaks in the spectra of Fig. 2. Errors represent one standard deviation from the fit values.

| $k$ (Å <sup>-1</sup> ) | $q_{\parallel \min}$ (Å <sup>-1</sup> ) | $q_{\parallel \max}$ (Å <sup>-1</sup> ) | $q_{\perp \min}$ (Å <sup>-1</sup> ) | $q_{\perp \max}$ (Å <sup>-1</sup> ) | BE (eV)    | BE* (eV)   |
|------------------------|---|---|-------------------------------------|-------------------------------------|------------|------------|
| $E_e = 15$ eV          |   |   |                                     |                                     |            |            |
| 0.34                   | 1.92                                    | 2.34                                    | 1.15                                | 1.81                                | 8.6 ± 0.2  | 2.6 ± 0.2  |
| 0.43                   | 1.92                                    | 2.35                                    | 1.11                                | 1.86                                | 14.9 ± 0.9 | 8.9 ± 0.9  |
| 0.51                   | 1.91                                    | 2.36                                    | 1.05                                | 1.90                                | 22.5 ± 0.7 | 16.5 ± 0.7 |
| 0.64                   | 1.90                                    | 2.36                                    | 0.95                                | 1.96                                | 29.8 ± 0.9 | 23.8 ± 0.9 |
| $E_e = 8$ eV           |   |   |                                     |                                     |            |            |
| 0.24                   | 1.69                                    | 2.06                                    | 0.82                                | 1.36                                | 9.3 ± 0.2  | 3.3 ± 0.2  |
| 0.34                   | 1.69                                    | 2.07                                    | 0.76                                | 1.39                                | 14.9 ± 0.3 | 8.9 ± 0.3  |
| 0.41                   | 1.68                                    | 2.07                                    | 0.72                                | 1.43                                | 20.4 ± 0.3 | 14.4 ± 0.3 |
| 0.55                   | 1.67                                    | 2.08                                    | 0.65                                | 1.53                                | 29.7 ± 0.6 | 23.7 ± 0.6 |

the observed transitions are substantially unchanged. The centroids of the individual Gaussian functions used to fit the corrected data of Fig. 2 are reported in Table I.

Both spectra of Fig. 2 are characterized by an intense peak at about 9 eV, accompanied by weaker structures at higher BE. Comparison with the calculated energy band structure<sup>25</sup> allows us to assign the main peak in the coincidence spectrum to the ionization of the  $\pi$  band. This peak is shifted by 0.7 eV towards lower BE and shows a larger width in the spectrum taken with  $E_e = 15$  eV. Both the shift and the broadening are ascribed to the  $\mathbf{q}$  dispersion of the  $\pi$  band, as the two kinematics sample different  $\mathbf{q}$  regions (see Table I). Accordingly, the second feature at 14.9 eV arises from unresolved contributions coming from the  $\sigma_3$  and  $\sigma_2$  bands, while the third feature (at 20.4 eV for  $E_e = 8$  eV and at 22.5 eV for  $E_e = 15$  eV) originates from  $\sigma_2$  and  $\sigma_1$ . However, the energy shift observed for the third peak is opposite to that expected on the basis of the calculated dispersion in the  $q_{\parallel}$  plane. Origin for this disagreement could be ascribed to the presence of a negative dispersion for  $\mathbf{q}$ 's characterized by parallel and perpendicular components, that are actually sampled by the experiment. For what concerns the high-energy part of the spectrum, it is conceivable to relate it to ionization from the  $\sigma_1$  band, the lowest one in graphite, though according to the results of Ref. 25 the measured binding energy is fairly larger than the calculated one. Intrinsic plasma excitation associated with the direct ionization of the  $\pi$  band<sup>27</sup> is an alternative explanation.

As far as the relative spectral intensities, they cannot be directly related to the momentum density of the band elec-

tron, because the kinematics of the present experiment do not satisfy the impulsive conditions, being intermediate between binary and dipolar regime. Furthermore, the PW approximation becomes questionable for the slow ejected electron. Its inadequacy is also indicated by the structured character observed in the spectrum of secondary electrons in the region 5–30 eV, as that is interpreted as reflecting the density of empty states of the crystal.<sup>28</sup> Basically the breakdown of the PWBA implies that the momentum balance in Eq. (4) is no longer rigorous, even though by replacing  $\mathbf{k}_e$  with a suitable wave packet a “range” of reconstructed  $\mathbf{q}$  can still be defined. It is on the basis of these considerations that the spectra of Fig. 2 were discussed by using energy and momentum conservation. They were found consistent with the picture of asymmetric ( $e,2e$ ) events due to direct ionization of the graphite valence bound states.

In conclusion the present work has clearly demonstrated the feasibility of coincidence ( $e,2e$ ) experiments in the reflection geometry. This arrangement is particularly suitable to study surface states, which makes the technique an attractive spectroscopy.

Further experimental work performed at higher ejected electron energy is under way in order to better fulfill the impulsive condition.

We are grateful to Progetto Finalizzato Chimica Fine of the CNR and to EEC Human Capital and Mobility, Contract No. ERBCHRXCT930350, for partial support of the work.

\*Present address: Dipartimento di Fisica, Università di Roma “La Sapienza,” Piazzale A. Moro 2, I-00185, Rome, Italy.

<sup>1</sup>G. Stefani, L. Avaldi, and R. Camilloni, in *New Directions in Research with Third Generation Soft X-ray Synchrotron Radiation Sources*, Vol. 254 of *NATO Advanced Study Institute: Series E*, edited by A. F. Schlachter and F. J. Wuilleumier (Kluwer Academic, Dordrecht, 1994), p. 161, and references therein.

<sup>2</sup>R. Camilloni, A. Giardini Guidoni, R. Tiribelli, and G. Stefani, *Phys. Rev. Lett.* **29**, 618 (1972).

<sup>3</sup>D. Voreades, *Surf. Sci.* **60**, 325 (1976).

<sup>4</sup>E. Weigold, *J. Phys. Colloq.* **3**, C6-187 (1993).

<sup>5</sup>J. Kirschner, O. M. Artamov, and A. N. Terekhov, *Phys. Rev. Lett.* **69**, 1711 (1992).

<sup>6</sup>M. Vos, P. Storer, S. A. Canney, A. S. Kheifets, I. E. McCarthy, and E. Weigold, *Phys. Rev. B* **50**, 5635 (1994).

<sup>7</sup>S. M. Thurgate, *Surf. Interface Anal.* **20**, 627 (1993).

<sup>8</sup>A. Hamnett, W. Stoll, G. Branton, C. E. Brion, and M. J. Van der Wiel, *J. Phys. B* **9**, 945 (1976).

<sup>9</sup>V. G. Levin, V. G. Neudachin, and Yu. F. Smirnov, *Phys. Status Solidi B* **49**, 489 (1972).

<sup>10</sup>L. Avaldi, R. Camilloni, E. Fainelli, and G. Stefani, *J. Phys. B* **20**, 4163 (1987).

<sup>11</sup>A. Ritter, J. R. Dennison, and R. Jones, *Phys. Rev. Lett.* **53**, 2054 (1984).

<sup>12</sup>P. Hayes, J. F. Williams, and J. Flexman, *Phys. Rev. B* **43**, 1928 (1991).

<sup>13</sup>S. Dey and J. F. Williams, *J. Phys. D* **21**, 108 (1988).

<sup>14</sup>C. Gao, A. Ritter, J. R. Dennison, and N. A. W. Holzwarth, *Phys. Rev. B* **37**, 3914 (1988).

<sup>15</sup>P. Hayes, M. A. Bennet, J. Flexman, and J. F. Williams, *Phys. Rev. B* **38**, 13 371 (1988).

<sup>16</sup>F. J. Pijper and P. Kruij, *Phys. Rev. B* **44**, 9192 (1991).

<sup>17</sup>J. Drucker, M. R. Scheinfein, J. Liu, and J. K. Weiss, *J. Appl. Phys.* **74**, 7329 (1993).

<sup>18</sup>A. D'Andrea and R. Del Sole, *Surf. Sci.* **71**, 306 (1978).

<sup>19</sup>D. L. Mills, *Surf. Sci.* **48**, 59 (1975).

<sup>20</sup>S. Iacobucci, P. Letardi, M. Montagnoli, P. Nataletti, and G. Stefani, *J. Electron Spectrosc. Relat. Phenom.* **67**, 479 (1994).

<sup>21</sup>H. Ehrhardt, K. Jung, G. Knoth, and P. Schlemmer, *Z. Phys. D* **1**, 3 (1986).

<sup>22</sup>R. Camilloni, S. Iacobucci, L. Marassi, S. Nannarone, and G. Stefani, *Vuoto* (to be published).

<sup>23</sup>R. G. Musket, W. Mc Lean, C. A. Colmenares, D. Makowiecki, and W. J. Siekhaus, *Appl. Surf. Sci.* **10**, 143 (1982).

<sup>24</sup>M. Cardona and L. Ley, in *Photoemission in Solids I*, edited by M. Cardona and L. Ley, *Topics in Applied Physics* Vol. 26 (Springer Verlag, Berlin, 1978), p. 1.

<sup>25</sup>R. C. Tatar and S. Rabii, *Phys. Rev. B* **25**, 4126 (1982).

<sup>26</sup>G. Ertl and J. Küppers, *Low Energy Electrons and Surface Chemistry*, 2nd ed. (Verlag Chemie, Monaco, 1985), p. 7.

<sup>27</sup>N. A. Krasil'Nikova and N. M. Persiantseva, *Phys. Lett.* **69A**, 287 (1978).

<sup>28</sup>L. S. Caputi, G. Chiarello, A. Santaniello, E. Colavita, and L. Papagno, *Phys. Rev. B* **34**, 6080 (1986).